ARTICLES

Persistence Length of Wormlike Micelles from Dynamic Light Scattering

Hans von Berlepsch,*,† Ludger Harnau,‡ and Peter Reineker‡

Max-Planck-Institut für Kolloid- und Grenzflächenforschung, Rudower Chaussee 5, D-12489 Berlin, Germany, and Abteilung Theoretische Physik, Universität Ulm, Albert-Einstein-Allee 11, D-89069 Ulm, Germany

Received: January 6, 1998; In Final Form: June 22, 1998

A theoretical model for the dynamic structure factor of semiflexible macromolecules has been applied to recently published dynamic light scattering measurements on dilute micellar solutions of the surfactant sodium sulfopropyl octadecyl maleate (SSPOM) in the presence of NaCl (von Berlepsch; et al. *Langmuir* **1996**, *12*, 3613). Good agreement between theory and experimental data is achieved when a persistence length of about 120 nm is assumed. The computed initial decay rate at large scattering vectors remains approximately unchanged if polydispersity is taken into account. Thus, by studying the dynamic structure factor at large scattering vectors, the persistence length of wormlike micelles can be extracted.

I. Introduction

Micelles formed by the aggregation of amphiphilic molecules in aqueous solution can grow dramatically under special conditions to form giant cylindrical aggregates.[1,2] If their length exceeds a characteristic length scale, known as the persistence length, they become flexible and resemble polymer molecules.[3,4] The self-assembling nature of the process of micelle formation leads to a broad distribution of aggregate lengths. Initially most experimental studies on elongated micelles were concerned with the characterization of micellar growth and structure.[2−4] However over the past decade the majority of studies have been dealing with more complex phenomena, such as rheological properties, multicomponent systems, isotropic-to-nematic transition, although a precise knowledge of micellar growth, bending elasticity, structure, and intermicellar interactions is still lacking.[5,6] In particular, quantitative data on the flexibility, or persistence length, of micelles is very limited because of difficulties in determining this parameter with high precision.[7] Early attempts have used simple crossover relations in the intermediate scattering vector range of small-angle neutron (SANS) and static light scattering (SLS) data[8−10] in order to estimate the persistence length. More recently fits of SLS data by polymer models such as that for wormlike chains[11−13] have been exploited to yield more reliable values. However, the chain flexibility is also reflected in the dynamic structure factor and thus should in principle be obtainable also from quasi-elastic neutron and dynamic light scattering (DLS) experiments. Because the theory of dynamics of semiflexible chains is generally much less developed, in most cases experimental data have been explained only qualitatively and again by using polymer models. Simple asymptotic relations have been used, which were derived for definite limiting cases, like flexible chains, stiff rods, or rods with dominating bending modes.[14−19] It has to be noted however that the modeling of dynamics of self-assembled aggregates is more complicated because the reversible scission and recombination processes leading to an equilibrium size distribution of the aggregates must be taken into account.[20] This was done by Cates et al.,[21] who discussed the dynamic structure factor of rodlike micelles at small scattering vectors where translational motion dominates. At present, corresponding calculations for elongated semiflexible and flexible micelles do not exist. It can be expected, however, that on a time scale shorter than the characteristic mean lifetime for scission or recombination, τ_b, the dynamic structure factor should be approximately describable by a quasi-quenched size distribution. If such an approximation is valid, a new detailed theory of the dynamic structure factor of semiflexible macromolecules with variable stiffness in dilute solution[22] can be used. Expressions for the initial decay rate of the dynamic structure factor, $\Gamma(Q)$, as a function of the scattering vector, Q, for arbitrary chain stiffnesses between the limits of flexible chains and stiff rods have been derived which allow quantitative estimates of the persistence length from experimental data. In the present paper this theory will be applied to fit experimental $\Gamma(Q)$ curves recently obtained by DLS on solutions of wormlike micelles.[13]

The considered surfactant sodium sulfopropyl octadecyl maleate (SSPOM) forms spheroidal micelles of a mean aggregation number of about 200 in aqueous solution. A spheroid-to-rod transition occurs after the addition of 80 mmol/L sodium chloride.[23] On further increasing of the salt concentration, the rods grow in length, becoming wormlike micelles of unusual high stiffness. The growth of the micelles was thoroughly investigated by light scattering, and the results have been discussed in detail in ref 13. There it was demonstrated that the concentration dependence of the normalized scattering intensity (Rayleigh ratio) obtained from SLS follows scaling laws below and above the crossover concentration, c^*, in quantitative agreement with theoretical predictions for rodlike micelles.[14,24] A corresponding scaling relation was found to hold for the hydrodynamic correlation length measured by DLS

† Max-Planck-Institut für Kolloid-und Grenzflächenforschung.
‡ Universität Ulm.

S1089-5647(98)00677-4 CCC: $15.00
Published on Web 09/09/1998

above c^*. Further it was observed that the apparent angular-dependent diffusion coefficient $\Gamma(Q)/Q^2$ for large scattering vectors Q, shows a power law behavior in the dilute concentration regime with exponents ranging between 0.45 and 0.60. These exponents fall within the range of values for flexible chains (exponent one, Zimm model) and stiff rods (exponent zero) and are closer to the value $^2/_3$ for straight rods with dominating bending fluctuations.[17] By applying the Koyama theory of wormlike chains, we could fit the angle dependence of the SLS data and estimated indeed a very large persistence length of about 120 nm at a temperature of 50 °C. In addition to the light scattering studies, SANS was used to characterize the cross-section structure of the micelles.[25]

With the available structural data, the SSPOM system appears to be a well-defined experimental model system for testing the theory of the dynamic structure factor. The present study was aimed at a quantitative description of the angle dependence of the former experimental DLS data by a theoretical approach which allows variable chain stiffness. The fit yields a persistence length agreeing with that from SLS. As expected, one has to consider effects arising from the polydispersity of micelles. A more detailed analysis of the latter problem will be given in a forthcoming theoretical paper.

II. Experiment and Methods

Light Scattering Experiments. DLS measurements were carried out using the instrument SIMULTAN (ALV, Langen, Germany), equipped with the correlator 5000, and a 400 mW YAG laser, $\lambda_0 = 532$ nm, as the light source. All measurements were performed at 50.0 ± 0.1 °C. The intensity autocorrelation functions were measured in steps of 10°, usually in the angle range between $\theta = 20$ and 150°, and individually analyzed using a second-order cumulant analysis.

After dissolution of the surfactant in aqueous solution containing 250 mmol/L NaCl at 60 °C, the samples were equilibrated for about 24 h at 55 °C and filtered directly into the scattering cells. More details of sample preparation may be found in ref 13. The measured correlation functions were monomodal in the dilute as well as in the semidilute concentration range. This finding and that of the long time necessary for equilibration of at least 24 h are important to note for the present investigation. They provide qualitative arguments which suggest that the measured correlation function reflects dominating cooperative diffusion processes, while the dynamics of reversible scission and recombination seems to be insignificant in the time domain explored in the experiment. The present system contrasts with other recent work on wormlike micelles, where a bimodal time correlation function with a Q-independent slow mode of viscoelastic origin was found.[26]

The measured intensity autocorrelation function was analyzed by a standard cumulant fit of second order, giving the first cumulant or initial decay rate, $\Gamma(Q)$, and the second cumulant, $\Gamma_2(Q)$, as fitting parameters. The absolute value of the scattering vector is given by $Q = (4\pi n/\lambda_0)\sin(\theta/2)$, where $n = 1.335$ is the index of refraction of the solution. The deviation of the correlation function from an exponential relation is expressed by the quantity Γ_2/Γ^2. For the system studied here typical values between 0.11 and 0.13 were obtained. For the dilute regime, i.e., surfactant concentrations, c, below the crossover concentration, c^*, we obtained four data sets for the apparent angular-dependent diffusion coefficient $D_{app}(Q) = \Gamma(Q)/Q^2$ vs Q. Likewise static light scattering on the same samples was performed under identical experimental conditions.

The experimental results, i.e., the scattering curves (SLS) and apparent diffusion coefficients (DLS) versus Q, as well as the reduced Rayleigh ratio extrapolated to zero scattering angle and the hydrodynamic correlation length as a function of surfactant concentration, respectively, are represented and discussed in ref 13 and are not reproduced here. For the crossover concentration a value of $c^* \approx 1 \times 10^{-3}$ g/mL has been estimated.

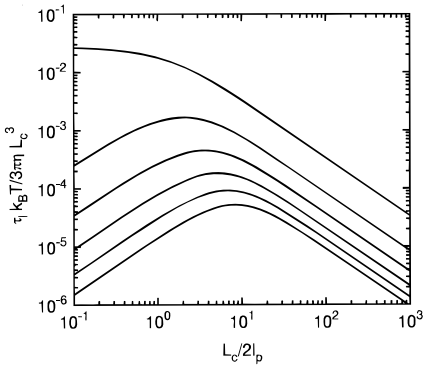

Figure 1. First six relaxation times τ_l as a function of $L_c/2l_p$. Mode number l increases from top to bottom. In the limit of $L_c/l_p \gg l\pi$ the relaxation times are proportional to L_c^2 and vary with l^{-2}, whereas in the limit of $L_c/l_p \ll l\pi$ and $l > 1$ the relaxation times are proportional to L_c^4 and exhibit a dependence $(2l-1)^{-4}$ on the mode number. The rotational relaxation time τ_1 is proportional to L_c^3 in the rod limit.

For a quantitative description of the results the measured SLS curves were fitted by the Koyama theory of wormlike chains, assuming a logarithmic distribution of chain lengths. The theoretical description yielded the weight-averaged micellar molecular mass M_w, persistence length l_p, contour length L_c, radius of gyration R_g, and the polydispersity index σ, where for the logarithmic distribution holds the following: $M_w/M_n = \exp(\sigma^2)$ with M_n the number-averaged micellar molecular mass. The influence of excluded-volume interactions may be neglected for concentrations below c^*. The mean radius of the cylindrical micelles was measured by SANS, giving 2.73 ± 0.27 nm.[25] These structure parameters are the input for the model calculations of the decay rate of the dynamic structure factor reported in the present paper.

Theory of Dynamic Structure Factor. According to the theory presented in ref 22, the dynamic structure factor is given by

$$S(Q,t) = \frac{e^{-Q^2Dt}}{L_c^2}\int_{-L_c/2}^{+L_c/2}\int_{-L_c/2}^{+L_c/2} ds\, ds'\, \exp\left(-\frac{Q^2}{6}a(s-s')\right) \times \exp\left(-\frac{Q^2 k_B T}{3\pi\eta}\sum_{l=1}^{\infty}\tau_l\psi_l(s)\,\psi_l(s')\left(1-\exp\left(-\frac{t}{\tilde{\tau}_l}\right)\right)\right) \quad (1)$$

with

$$a(s-s') = 2|s-s'|l_p - 2l_p^2\left(1-\exp\left(\frac{-|s-s'|}{l_p}\right)\right) \quad (2)$$

where D is the translational diffusion coefficient which exhibits a length dependence $D \sim 1/L_c^{1/2}$ for flexible chains and $D \sim \ln L_c/L_c + \text{constant}/L_c$ for stiff rods. The temperature, T, and viscosity, η, characterize the solvent. $\psi_l(s)$ are the eigenfunctions (eqs 2.22−2.24 of ref 22) of the normal-mode analysis describing the intermolecular dynamics. The corresponding eigenvalues are characterized by the relaxation times τ_l, where l is the mode number.[27] The first six relaxation times τ_l are plotted in Figure 1 as a function of $L_c/2l_p$. For relaxation times τ_l, $l > 1$, three regimes are distinguishable. For $L_c/l_p \gg l\pi$ the relaxation times are proportional to L_c^2 and vary as l^{-2},

representing the stretching modes of the well-known Rouse model. The Rouse model considers the macromolecules as self-similar random walks.[28] In the limit of $L_c/l_p \ll l\pi$ the relaxation times are proportional to L_c^4 and exhibit the dependence $(2l-1)^{-4}$ on the mode number, as known for the bending modes of the model of Aragón and Pecora,[29] resulting in a wider distribution of the relaxation times in this limit. In the intermediate regime both bending and stretching contribute to the relaxation times. It should be noted that the calculations yield a crossover from intramolecular stretching to bending modes with increasing mode number even for very flexible chains due to finite chain stiffness. This reflects the fact that a wormlike chain appears increasingly stiff on smaller length scales. The first relaxation time τ_1 exhibits the typical Rouse behavior. For stiff rods the well-known relation $\tau_1 \sim L_c^3$ is found.

The hydrodynamic interaction is included in the calculation of the intramolecular dynamics in terms of the relaxation times $\tilde{\tau}_l$ which are calculated using the Rotne−Prager tensor.[30] The influence of the hydrodynamic interaction on the relaxation times for wormlike chains becomes more dominant with both increasing chain flexibility and increasing mode number l. In evaluating the dynamic structure factor according to eq 1, it is found that at scattering vectors larger than the inverse persistence length the chain stiffness is important for any kind of chain, i.e., even for very flexible ones. Both the shape of the dynamic structure factor and the initial decay rate, $\Gamma(Q)$, defined by

$$\ln(S(Q,t)/S(Q,0)) = -\Gamma(Q)t + \Gamma_2(Q)\frac{t^2}{2} - \ldots \qquad (3)$$

differ from the results known for flexible chains. In particular the Q-dependence of $\Gamma(Q)$ is weaker than that predicted by the Zimm model for flexible chains ($\Gamma(Q) \sim Q^3$). The Zimm model is an extension of the Rouse model including hydrodynamic interaction.[28] The comparison of the theoretical calculations with quasi-elastic neutron and dynamic light scattering measurements on various natural and synthetic macromolecules such as denaturated ovalbumin, DNA, *F*-actin, gellan and polystyrene in dilute solution exhibits good agreement.[22,31] At large scattering vectors $QR_g > 3$, the relation $\Gamma(Q) \sim Q^\beta$ with $\beta = 2.75$ for DNA ($L_c/2l_p = 10$) and $\beta = 2.56$ for gellan ($L_c/2l_p = 1.9$) is approximately valid. Details concerning the model calculations may be found in ref 22.

For a solution containing wormlike chains of different chain lengths the dynamic structure factor is given by

$$S_z(Q,t) = \frac{\int_0^\infty \mathrm{d}L_c\, S(Q,t)\, w(L_c) L_c}{\int_0^\infty \mathrm{d}L_c\, w(L_c) L_c} \qquad (4)$$

where $w(L_c)$ is the length distribution. Thus the dynamic structure factor is calculated as a function of contour length, and the result is then averaged over the (quasi-quenched) length distribution. In general, the shape of the dynamic structure factor at large scattering vectors is only slightly influenced by polydispersity since local motion on a small length scale is independent of the contour length. The effect of polydispersity on the apparent diffusion coefficient $\Gamma(Q)/Q^2$ at small scattering vectors for wormlike macromolecules has already been discussed by Schmidt.[32]

III. Results and Discussion

The measured apparent diffusion coefficients $\Gamma(Q)/Q^2$ of four dilute concentrations ($c < c^*$) are plotted in a normalized form in Figure 2. The error bars are also shown. All data points (symbols) fall in rough approximation onto the same theoretical curve (solid line). However, before discussing the quality of the fit, the required model parameters and their estimation from the corresponding SLS data will be considered.

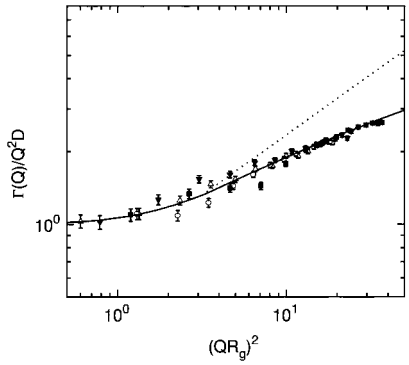

Figure 2. log−log plot of the normalized initial decay rate $\Gamma(Q)/Q^2D$ according to eq 3 for $L_c/2l_p = 2.1$ (solid line). The dotted line corresponds to the relation $\Gamma(Q) \sim Q^3$. The symbols display experimental data on SSPOM micelles in dilute NaCl (250 mmol/L) solution at different surfactant concentrations (g/mL): ■, 1×10^{-4}; ▼, 1.8×10^{-4} ; ○, 3×10^{-4}; △, 5×10^{-4}.

TABLE 1: Micellar Molecular Mass M_w, Contour Length L_c, Radius of Gyration R_g, and Polydispersity Index σ of SSPOM Micelles at 250 mmol/L NaCl and 50 °C from SLS[13]

c (g/mL)	M_w (10^6 g/mol)	L_c (nm)	l_p (nm)	R_g (nm)	σ
1×10^{-4}	6.31	598	125	200	0.85
1.8×10^{-4}	7.19	573	115	162	0.70
3×10^{-4}	6.14	440	125	140	0.70
5×10^{-4}	9.17	593	119	142	0.50

Starting with the micellar molecular mass M_w, it should be noted that a scaled plot of the reduced osmotic compressibility constructed from the raw SLS data (see Figure 14a of ref 13) yielded an exponent $\alpha = 0.45$ for the "growth" law $M_w \sim c^\alpha$ in good agreement with the mean field theory of linear micelles[1,20] (for flexible chains in dilute solution $\alpha = 0.46$ holds[24,33]). All micelle characteristics for the four different concentrations obtained from fits of the single SLS curves by the Koyama theory of wormlike chains are summarized in Table 1 (see Table 2 in ref 13). Micellar molecular mass M_w, contour length L_c, and radius of gyration R_g show some scatter. A tendency for micellar growth beyond the scatter is obvious only from the M_w data and indicates the micellar size increase. As flexibility and polydispersity are correlated parameters and a fixed persistence length seems physically reasonable, all SLS curves were fitted using the same persistence length and a slight scatter in polydispersity was obtained, as indicated in Table 1. The interactions between the micelles are weak and have been neglected in Koyama theory and also for the present calculations. The influence of excluded-volume interactions increases with c and has been estimated by calculating the second virial coefficient of rodlike particles in ref 13. The correction terms obtained are positive so that the real masses increase more strongly with concentration, as expected. The limits of error reaching 12% at $c = 5 \times 10^{-4}$ g/mL seem acceptable. The tabulated radii of gyration R_g are used to calculate the reduced scattering vector (QR_g) in the normalized plot of Figure 2.

We return to the modeling of the apparent diffusion coefficient $\Gamma(Q)/Q^2$. The four available data sets were each fitted with the parameters given in Table 1. The fitting universal curve (solid line) of Figure 2 was computed according to eq 3 for $L_c/2l_p = 2.1$. The universality is physically consistent under the assumption of a fixed persistence length when micellar

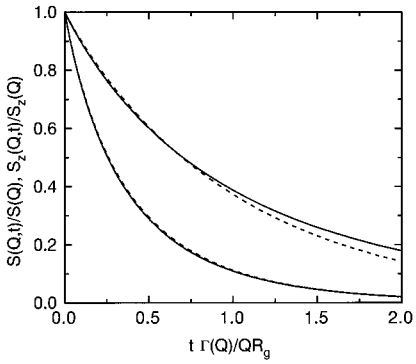

Figure 3. Normalized dynamic structure factor for scattering vectors $QR_g = 1$ (upper curves) and $QR_g = 3$ (lower curves). The dashed curves are computed for monodisperse chains with $L_c = 593$ nm and $l_p = 120$ nm according to eq 1. The solid curve represents the normalized dynamic structure factor for polydisperse chains with a polydispersity index $\sigma = 0.8$ according to eq 4. $\Gamma(Q)$ is the initial decay rate for monodisperse chains.

growth is weak. To check the sensitivity of the parameter $L_c/2l_p$ to the measured data, decay rates for a range of l_p-values were calculated, revealing that a 10% variation of the $L_c/2l_p$-value changes the decay rates by about 2%. As the experimental data points show the same level of error at least in the large Q-range, an error limit of about 10% for the fitted persistence length l_p is estimated. The larger deviations between experimental data and theory appearing in the low-angle range originate most probably from the polydispersity and will be discussed below. The calculation verifies nicely the former estimate $l_p \approx 120$ nm from SLS. It is obvious that the overall translational motion is dominant in the low scattering vector regime $QR_g < 1$, confirming the relation $\Gamma(Q) = Q^2D$. For larger scattering vectors $QR_g > 1$, the internal modes dominate and the decay rate is no longer proportional to the square of the scattering vector. As apparent from Figure 2, there is no intermediate scattering vector regime in which the relation $\Gamma(Q) \sim Q^3$ holds. Furthermore, a simplified analysis in terms of bending modes only also yields an incorrect Q-dependence, as noted in the Introduction. As is obvious from Figure 1 the $L_c/2l_p$-value of the micelles is in the range where both bending and stretching modes contribute to the relaxation times. Hence, models using either bending modes or stretching modes only fail to describe the experimental data. Consequently, it is necessary to include both, as suggested by the theory presented in ref 22.

The deviation of the experimental data points from the theoretical curve increases with decreasing scattering vector. There are two possible reasons for this behavior. One is the increasing experimental error in the low-angle range,[13] and the other is the polydispersity. The solid curve in Figure 2 is calculated for monodisperse chains. To study the polydispersity effect on the DLS data, the dynamic structure factor was calculated according to eq 4 for various degrees of polydispersity. Figure 3 represents the normalized dynamic structure factor for scattering vectors $QR_g = 1$ and $QR_g = 3$. For the polydisperse case a logarithmic length distribution with $\sigma = 0.8$ and the weight-average contour length $L_c = 593$ nm is used. The polydispersity index $\sigma = 0.8$ corresponds to $M_w/M_n = 1.9$, which is a typical value for wormlike micelles.[1,20] The persistence length $l_p = 120$ nm is fixed. As is obvious from Figure 3 only a small effect of the polydispersity is found on the shape of the dynamic structure factor at the scattering vector $QR_g = 3$. This also holds for scattering vectors $QR_g > 3$ and is independent of the used length distribution function. A Schulz−Zimm distribution with polydispersity $M_w/M_n = 2$ (equivalent to the theoretically predicted[20] exponential number density distribution of micelle lengths) gives an indistinguishable curve in that Q-range. Thus, local dynamics is independent of the contour length, as pointed out earlier. However, polydispersity influences the dynamic structure factor at a scattering vector $QR_g = 1$, where the translational diffusion is dominant. The deviation between the dynamic structure factor for monodisperse chains and polydisperse chains increases with increasing time. Therefore it can be concluded that the polydispersity effect would change the computed results for $QR_g < 3$ in Figure 2 by less than 5%. A detailed study of the influence of polydispersity on DLS data will be presented elsewhere.

IV. Conclusions

The dynamic light scattering data of SSPOM micelles are well-reproduced by the theory of dynamic structure factor of semiflexible macromolecules assuming a persistence length of about 120 nm. This persistence length quantitatively confirms the recent estimate from static light scattering. Also it should be emphasized that the computed initial decay rate at large scattering vectors $QR_g > 3$ remains approximately unchanged if polydispersity is taken into account. Thus, by studying the dynamic structure factor at large scattering vectors, the persistence length of wormlike micelles can be extracted. The excellent agreement between the persistence lengths estimated from both static and dynamic light scattering supports subsequently the initial assumption of a quasi-quenched size distribution for the investigated experimental system.

Acknowledgment. H.v.B. is grateful to H. Dautzenberg for the help with the experiments and to P. van der Schoot for valuable discussions. The theoretical investigations are part of a project of the Sonderforschungsbereich 239. The support of the Deutsche Forschungsgemeinschaft is gratefully acknowledged. Finally, we gratefully acknowledge the essential theoretical contributions of R. G. Winkler.

References and Notes

(1) Israelachvili, J. N.; Mitchell, D. J.; Ninham, B. W. *J. Chem. Soc., Faraday Trans. 2* **1976**, *72*, 1525.

(2) Mazer, N. A.; Benedek, G. B.; Carey, M. C. *J. Phys. Chem.* **1976**, *80*, 1075.

(3) Porte, G.; Appel, J.; Poggi, Y. *J. Phys. Chem.* **1980**, *84*, 3105.

(4) Candau, S. J.; Hirsch, E.; Zana, R. *J. Phys. (Paris)* **1984**, *45*, 1263.

(5) Odijk, T. *Curr. Opin. Colloid Interface Sci.* **1996**, *1*, 337.

(6) Schurtenberger, P. *Curr. Opin. Colloid Interface Sci.* **1996**, *1*, 773.

(7) Magid, L. In *Dynamic Light Scattering. The Method And Some Applications*; Brown, W., Ed.; Monographs on the Physics and Chemistry of Materials; Clarendon Press: Oxford, U.K., 1993; Vol. 49, p 555.

(8) Marignan, J.; Appell, J.; Bassereau, P.; Porte, G.; May, R. P. *J. Phys. (Paris)* **1989**, *50*, 3553.

(9) Schurtenberger, P.; Magid, L. J.; King, S.; Lindner, P. *J. Phys. Chem.* **1991**, *95*, 4173.

(10) Butler, P. D.; Magid, L. J.; Hayter, J. B. In *Structure and Flow in Surfactant Solutions*; Herb, C. A., Prud'homme, R. K., Eds.; ACS Symposium Series 578; American Chemical Society: Washington, DC, 1994; p 250.

(11) Denkinger, P.; Burchard, W.; Kunz, M. *J. Phys. Chem.* **1989**, *93*, 1428.

(12) Schurtenberger, P.; Cavaco, C. *Langmuir* **1994**, *10*, 100.

(13) von Berlepsch, H.; Dautzenberg, H.; Rother, G.; Jäger, J. *Langmuir* **1996**, *12*, 3613.

(14) de Gennes, P. G. *Scaling Concepts in Polymer Physics*; Cornell University Press: Ithaca, NY, 1979.

(15) Burchard, W.; Schmidt, M.; Stockmayer, W. H. *Macromolecules* **1980**, *13*, 580.

(16) Candau, S. J.; Hirsch, E.; Zana, R. *J. Colloid Interface Sci.* **1985**, *105*, 521.

(17) Farge, E.; Maggs, A. C. *Macromolecules* **1993**, *26*, 5041.
(18) Schurtenberger, P.; Cavaco, C. *J. Phys. Chem.* **1994**, *98*, 5481.
(19) Herzog, B.; Huber, K.; Rennie, A. R. *J. Colloid Interface Sci.* **1994**, *164*, 370.
(20) Cates, M. E.; Candau, S. J. *J. Phys.: Condens. Matter* **1990**, *2*, 6869.
(21) Cates, M. E.; Marques, C. M.; Bouchaud, J.-P. *J. Chem. Phys.* **1991**, *94*, 8529.
(22) Harnau, L.; Winkler, R. G.; Reineker, P. *J. Chem. Phys.* **1996**, *104*, 6355.
(23) von Berlepsch, H.; Stähler, K.; Zana, R. *Langmuir* **1996**, *12*, 5033.
(24) van der Schoot, P. *Europhys. Lett.* **1997**, *39*, 25.
(25) von Berlepsch, H.; Mittelbach, R.; Hoinkis, E.; Schnablegger, H. *Langmuir* **1997**, *13*, 6032.
(26) Buhler, E.; Munch, J. P.; Candau, S. J. *J. Phys. II (Paris)* **1995**, *5*, 765.
(27) Harnau, L.; Winkler, R. G.; Reineker, P. *J. Chem. Phys.* **1995**, *102*, 7750.
(28) Doi, M.; Edwards, S. F. *The Theory of Polymer Dynamics*; Clarendon: Oxford, U.K., 1986.
(29) Aragón, S.; Pecora, R. *Macromolecules* **1985**, *18*, 1868.
(30) Rotne, J.; Prager, S. *J. Chem. Phys.* **1969**, *50*, 4831.
(31) Harnau, L.; Winkler, R. G.; Reineker, P. *Macromolecules* **1997**, *30*, 6974.
(32) Schmidt, M. *Macromolecules* **1984**, *17*, 553.
(33) Wittmer, J. P.; Milchev, A.; Cates, M. E. *Europhys. Lett.* **1998**, *41*, 291.